Supporting information for:

Influence of Alkyl Chain Fluorination Proportion on the Photovoltaic Performance of Non-Fullerene Acceptors

Shuai Liu,[a] Tongzi Li,[a] Xiaoli Zhou,[a] Wenting Liang,[a] Shenbo Zhu,[a] Wenzhao Xiong,[a] Yongjie Cui,[a] Huawei Hu,[*a] Yiwang Chen[*a]

[a] State Key Laboratory for Modification of Chemical Fibers and Polymer Materials, College of Materials Science and Engineering, Donghua University, Shanghai 201620, China.

E-mail: huaweihu@dhu.edu.cn, ywchen@ncu.edu.cn

Molecular properties characterization (UV-vis spectra, TGA, and CV):

The UV-Vis absorption spectra of the solution and film were acquired on a Shimadzu UV-1200 Spectrophotometer. Film samples were spin-cast on ITO substrates. Thermogravimetric analysis (TGA) was carried out on a WCT-2 thermal balance under nitrogen protection at a heating rate of 10 ^{o}C/min. UV-Vis absorption spectra were collected from the solution of the two polymers with a concentration of 0.02 mg/mL in chloroform at different temperatures. Cyclic voltammetry was carried out on a Interface1000E electrochemical workstation with three electrodes configuration, using Ag/AgCl as the reference electrode, a Pt plate as the counter electrode, and a glassy carbon as the working electrode, in a 0.1 mol/L tetrabutylammonium hexafluorophosphate acetonitrile solution. Potentials were referenced to the ferrocenium/ferrocene couple by using ferrocene as external standards in acetonitrile solutions. The HOMO energy levels were determined by $E_{HOMO} = -[q\,(E_{re} - E_{ferrocene}) + 4.8\ eV]$, while the LUMO energy levels were determined by $E_{LUMO} = -[q\,(E_{ox} - E_{ferrocene}) + 4.8\ eV]$.

Fabrication and testing of Polymer:SMA devices: The best performance for the polymer:SMA devices was achieved after extensive optimization with an inverted structure of ITO/2PACz/polymer:SMA/PNDIT-F_3N/Ag and the details are as follows. Pre-patterned ITO-coated glass with a sheet resistance of ~15 Ω per square was used as

the substrate. It was cleaned by sequential sonication in soap DI water, DI water, acetone and isopropanol for 15 min at each step. After ultraviolet/ozone treatment for 60 min, a 2PACz hole transport layer was prepared by spin coating at 4000 r.p.m. Active layers were spin coated from the polymer: NFAs solution to obtain thicknesses of ~100 nm. Polymer: NFAs active layers were cast from chloroform solution (0.75 vol% CN as additive) with 7 mg/mL polymer concentration and 1:1.2 D/A ratio. The thermally annealed polymer: NFAs films were then annealed at 100 ^{o}C for 10 min followed by spin coating of a thin layer of PNDIT-F_3N. Then the substrates are transferred to the vacuum chamber of a thermal evaporator inside the glove box and 100 nm of Ag was deposited as the top electrode. All cells were measured inside the glove box. For device characterizations, *J-V* characteristics were measured under AM1.5G light (100 mWcm^{-2}) using a Class AAA Newport solar simulator. The light intensity was calibrated using a standard Si diode (with KG5 filter, purchased from PV Measurement) to bring spectral mismatch to unity. *J-V* characteristics were recorded using a Keithley 236 source meter unit.

Electron and hole mobility measurements. The electron mobilities were measured using the SCLC method, employing a device architecture of ITO/ZnO/active layer /PNDIT-F3N/Ag The hole-mobilities were measured using a device architecture of ITO/PEDOT:PSS/active layer/MoO_3/Ag. The mobilities were obtained by taking current-voltage curves and fitting the results to a space charge limited form, where the SCLC is described by:

$$J = \frac{9\varepsilon_0\varepsilon_r\mu(V_{\mathrm{appl}} - V_{\mathrm{bi}} - V_s)^2}{8L^3}$$

Where ε_0 is the permittivity of free space, ε_r is the relative permittivity of the material (assumed to be 3), μ is the hole mobility and L is the thickness of the film. From the plots of $J^{1/2}$ vs $V_{\mathrm{appl}} - V_{\mathrm{bi}} - V_s$, electron mobilities can be deduced.

AFM characterization: AFM measurements were performed by using a Scanning Probe Microscope Dimension 3100 in tapping mode. All film samples were spin-cast on ITO substrates.

GIWAXS characterization: GIWAXS measurements were performed at beamline BL16B1 at the Shanghai Synchrotron Radiation Facility. Samples were prepared on Si substrates using identical blend solutions as those used in devices. The 10 KeV X-ray beam was incident at a grazing angle of 0.13°, which maximized the scattering intensity from the samples. The scattered X-rays were detected using a Dectris Pilatus 1-M photon counting detector. Samples were prepared on Si substrates. In-plane and out-of-plane sector averages were calculated using the Nika software package. The uncertainty for the peak fitting of the GIWAXS data is 0.3 Å. The coherence length was calculated using the Scherrer equation: $CL=2\pi K/\Delta q$, where Δq is the full-width at half-maximum of the peak and K is a shape factor (0.9 was used here).[1]

Surface Energy: Contact angle measurements were carried out by an Attension Theta Flex meter, using water and ethylene glycol by sessile drop analysis. The solution of each pure organic material was spin-coated on cleaned ITO substrates. Droplets of two different liquids, water and ethylene glycol (EG) were cast onto the pure organic films with the drop size kept at 4 µL per drop. Contact angle images were taken at 1 s after the whole droplet was deposited onto the sample surface. At least 3 independent measurements were performed for each single liquid. The surface tension values of films are calculated according to the previous report[2], in which:

$$\gamma_{Water}(\cos\theta_{Water} + 1) = \frac{4\gamma_{water}^{p}\times\gamma^{p}}{\gamma_{water}^{p}+\gamma^{p}} + \frac{4\gamma_{water}^{d}\times\gamma^{d}}{\gamma_{water}^{d}+\gamma^{d}}$$

$$\gamma_{EG}(\cos\theta_{EG} + 1) = \frac{4\gamma_{EG}^{p}\times\gamma^{p}}{\gamma_{EG}^{p}+\gamma^{p}} + \frac{4\gamma_{EG}^{d}\times\gamma^{d}}{\gamma_{EG}^{d}+\gamma^{d}}$$

$$\gamma = \gamma^{d} + \gamma^{p}$$

where θ is the contact angle of each thin film, and γ is the surface tension of samples, which is equal to the sum of the dispersion (γ^{d}) and polarity (γ^{p}) components; γ_{water}

and γ_{EG} are the surface tensions of the water and ethylene glycol; and γ^d_{water}, γ^p_{water}, γ^d_{EG} and γ^p_{EG} are the dispersion and polarity components of γ_{Water} and γ_{EG}.

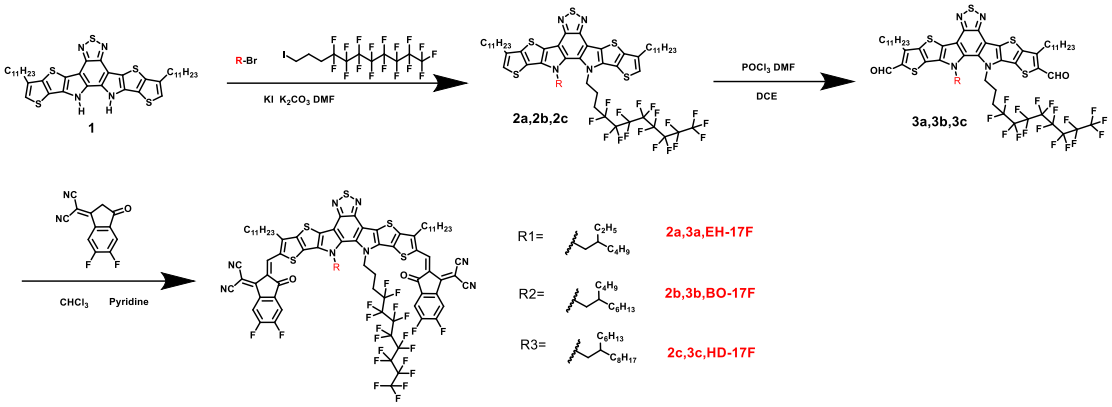

Scheme S1. Synthetic route for EH-17F, BO-17F and HD-17F.

Table S1. Basic parameters for EH-17F, BO-17F, and HD-17F.

Materials	λ_{max} [a] [nm]	λ_{max} [b] [nm]	λ_{onset} [b] [nm]	E_g^{opt} [c] [eV]	LUMO/HOMO [d] [eV]	T_d [°C]
EH-17F	722	803	859	1.44	-3.93/-5.68	346.0
BO-17F	722	805	861	1.44	-3.93/-5.69	347.4
HD-17F	722	810	858	1.45	-3.94/-5.68	343.3

[a] In solution state (Chloroform). [b] In pure films. [c] Obtained with $E_g^{opt} = 1240/\lambda_{onset}$ [b]. [d] Measured by cyclic voltammetry (CV) method.

Table S2. Device Performance based on PM6:EH-17F with different D/A ratios.

D/A ratio (wt/wt)	V_{OC} (V)	J_{SC} (mA cm^{-2})	FF (%)	PCE (%)
1.0:1.0	0.82	23.5	53.4	10.3
1.0:1.2	0.83	24.1	54.5	10.9
1.0:1.5	0.83	23.7	54.0	10.6

Table S3. Device Performance based on PM6:EH-17F with different amount of CN additive.

CN (vol%)	V_{OC} (V)	J_{SC} (mA cm^{-2})	FF (%)	PCE (%)
0	0.84	22.5	50.9	9.6
0.25	0.83	23.6	52.9	10.4
0.50	0.83	23.7	53.7	10.6
0.75	0.83	24.1	54.5	10.9
1.00	0.83	24.0	53.5	10.7

Table S4. The electrical parameters for corresponding devices.

	P_{diss}	P_{coll}	α	n
PM6: EH-17F	94.3	73.6	0.97	1.39
PM6: BO-17F	96.6	80.4	0.98	1.37
PM6: HD-17F	96.9	80.9	0.99	1.18

Table S5. The charge mobility of hole or electron-only devices for corresponding blend films.

	μ_h (10^{-4} cm^2 V^{-1} s^{-1})	μ_e (10^{-4} cm^2 V^{-1} s^{-1})	μ_h/μ_e
PM6: EH-17F	1.9	0.8	2.46
PM6: BO-17F	2.9	2.2	1.32
PM6: HD-17F	3.9	3.2	1.26

Table S6. Detailed energy loss analysis of OSCs devices.

Active layer	E_g (eV)	$V_{oc,sq}$ (V)	ΔE_1 (eV)	ΔE_2 (eV)	ΔE_3 (eV)	E_{loss} (eV)	E_U (meV)
PM6: EH-17F	1.433	1.169	0.264	0.053	0.286	0.603	24.3
PM6: BO-17F	1.429	1.167	0.262	0.051	0.276	0.589	24.0
PM6: HD-17F	1.439	1.176	0.263	0.048	0.268	0.579	23.9

[a)] $V_{oc,sq}$: Schokley–Queisser limit to V_{OC}. [b)] $V_{oc,rad}$: V_{OC} when there is only radiative recombination.

Table S7. Parameters of out-of-plane π-π stacking for donor and acceptor in the corresponding films.

	Direction	q (Å^{-1})	d (Å)	CCL(Å)
EH-17F	OOP	1.74	3.61	34.3
	IP	0.27	23.26	51.4
BO-17F	OOP	1.74	3.61	33.9
	IP	0.28	22.43	55.6
HD-17F	OOP	1.74	3.61	31.4
	IP	0.29	21.66	62.8
PM6:EH-17F	OOP	1.74	3.61	27.7
	IP	0.27	23.27	80.8
PM6:BO-17F	OOP	1.73	3.62	30.4
	IP	0.28	22.43	86.3
PM6:HD-17F	OOP	1.73	3.62	30.1
	IP	0.28	22.43	90.1

Table S8. Surface characteristics parameters.

Films	Contact angle (°)		γ_s^d	γ_s^p	γ_s	X^{D-A}
	H_2O	EG	(mJ m^{-2})	(mJ m^{-2})	(mJ m^{-2})	(k)
PM6	102.5	75.0	25.5	0.5	26.0	-
EH-17F	116.5	96.5	12.5	0.3	12.8	2.3
BO-17F	115.4	93.2	15.5	0.1	15.6	1.3
HD-17F	108.6	86.5	16.6	0.7	17.3	0.9

[a] γ_s^d is the dispersion component of surface free energy; [b] γ_s^p is the polar component of surface free energy; [c] γ_s is surface free energy; [d] χ_{D-A} is Flory-Huggins interaction parameters.

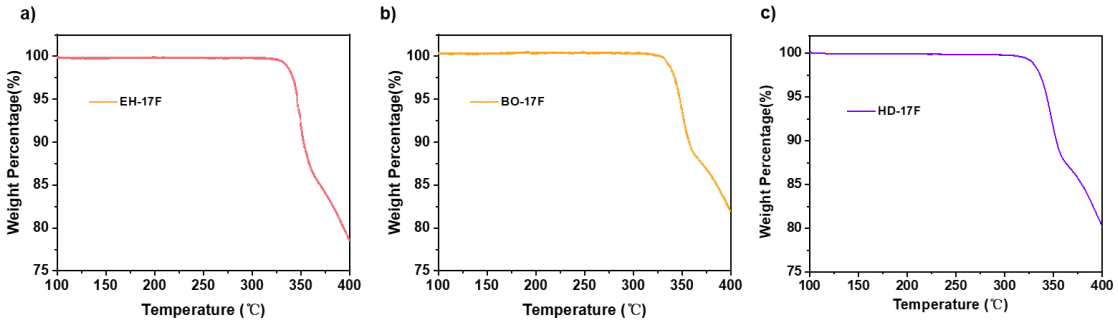

Figure S1. Thermogravimetric analysis (TGA) curve of (a) EH-17F, (b) BO-17F, and (c) HD-BO measured with a heating rate of 10 ^oC/ min under N_2 atmosphere.

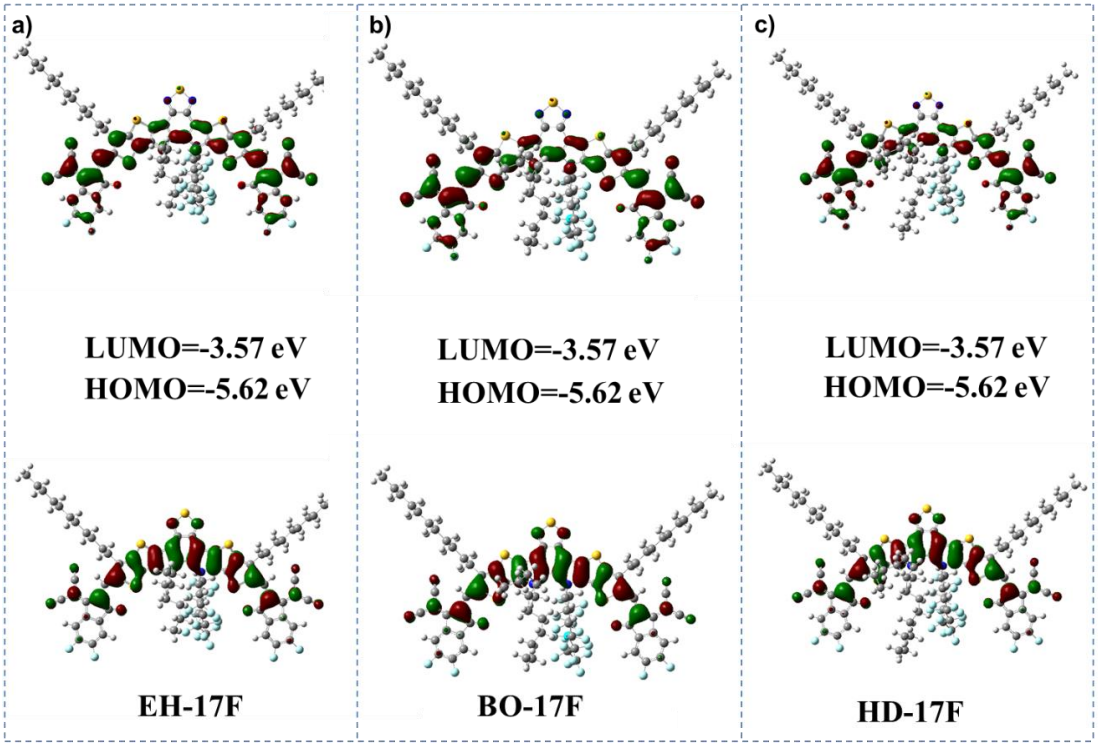

Figure S2. the HOMO and LUMO energy levels of (a) EH-17F, (b) BO-17F, and (c) HD-BO.

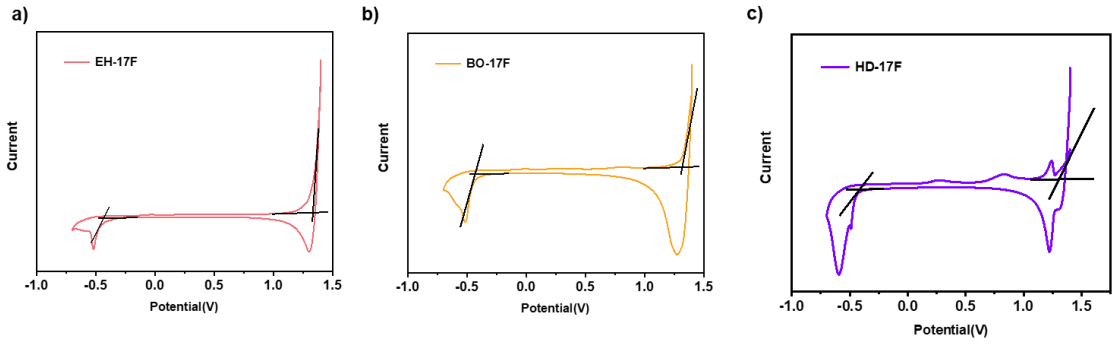

Figure S3. The CV plots of (a) EH-17F, (b) BO-17F, and (c) HD-BO.

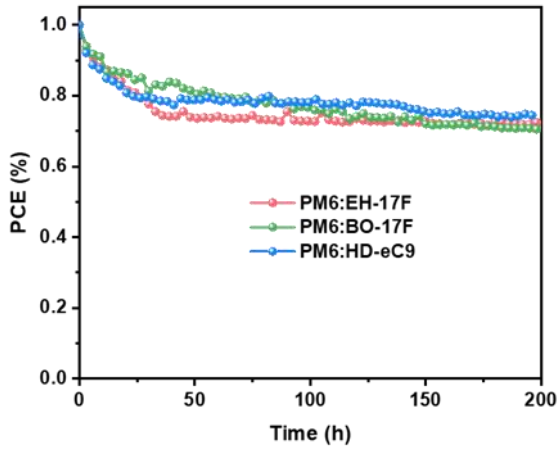

Figure S4. Photostability of the encapsulated devices with MPP tracking under 1-sun illumination.

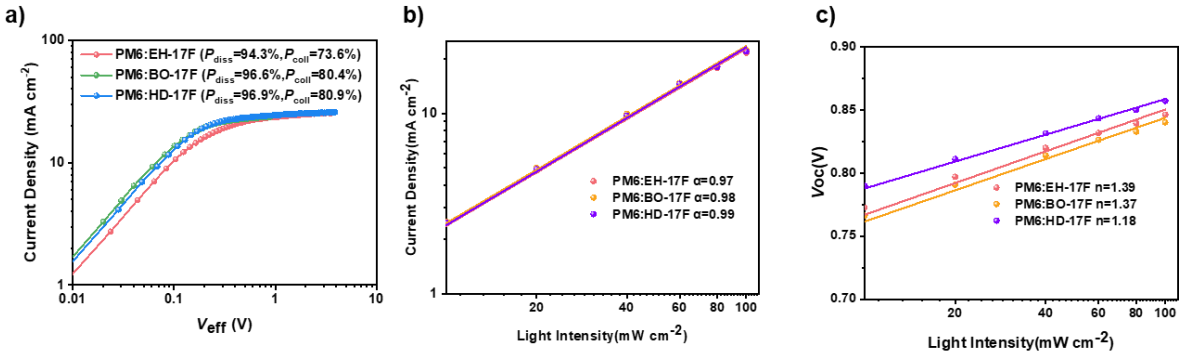

Figure S5. (a) J_{ph}–V_{eff} relationships. Light intensity dependence of the (b) short-circuit current density and (c) open-circuit voltage and of the OSC.

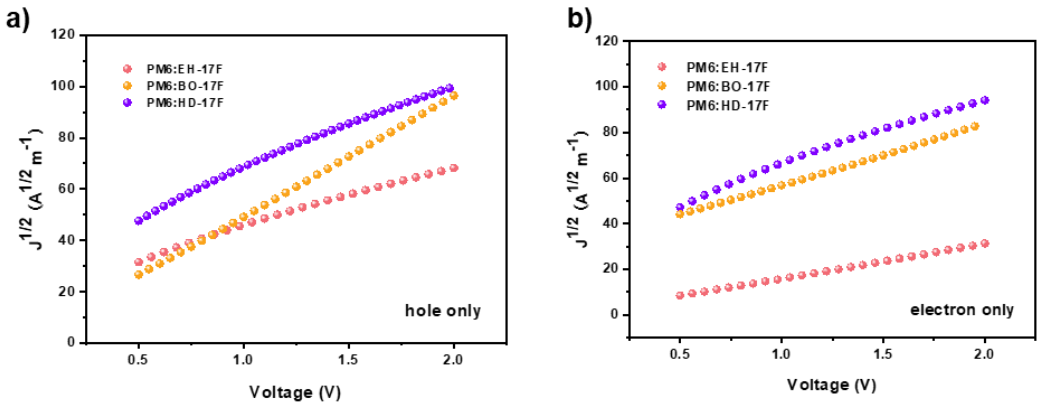

Figure S6. (a) Hole and (b) Electron current densities with applied voltage in selective carrier injected diodes.

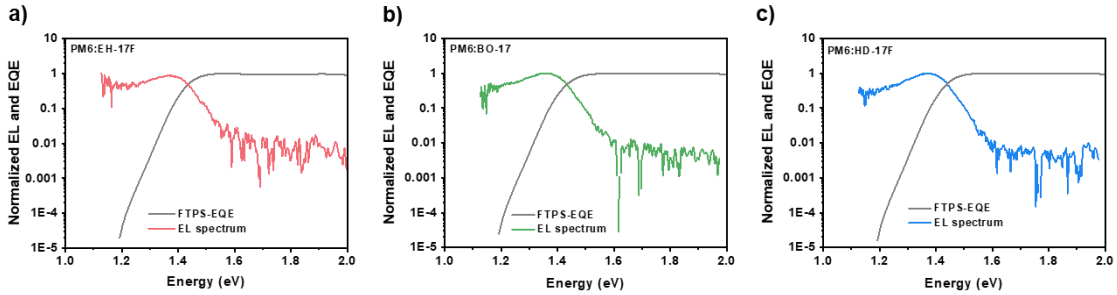

Figure S7. Semilogarithmic plots of normalized FTPS-EQE and EL as a function of energy for (a) PM6:EH-17F, (b) PM6:BO-17F, and (c) PM6:HD-17F-based devices.

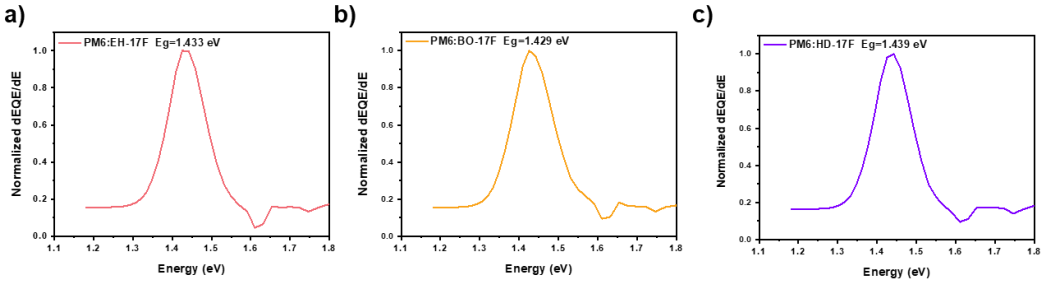

Figure S8. Details of optical Eg determination calculated from the derivatives of the FTPS−EQE curves.

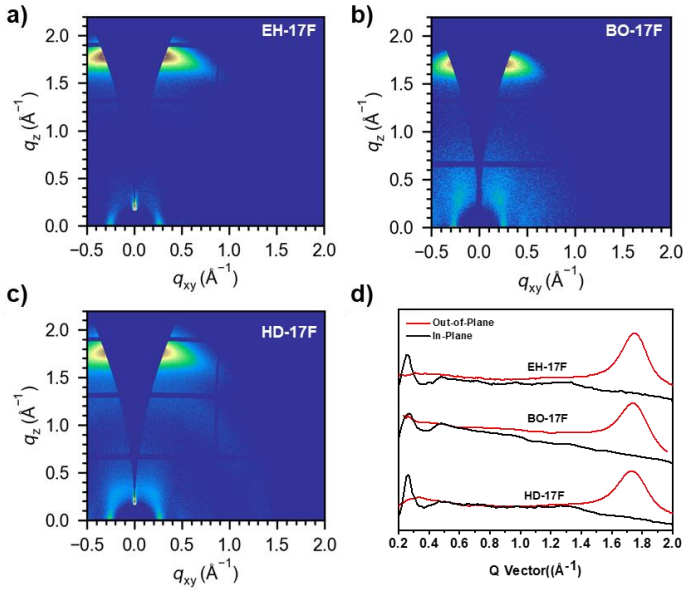

Figure S9. 2D GIWAXS patterns for (a) EH-17F, (b) BO-17F, and (c) HD-BO. (d) out-of-plane and in-plane GIWAXS profiles for neat NFA-based films.

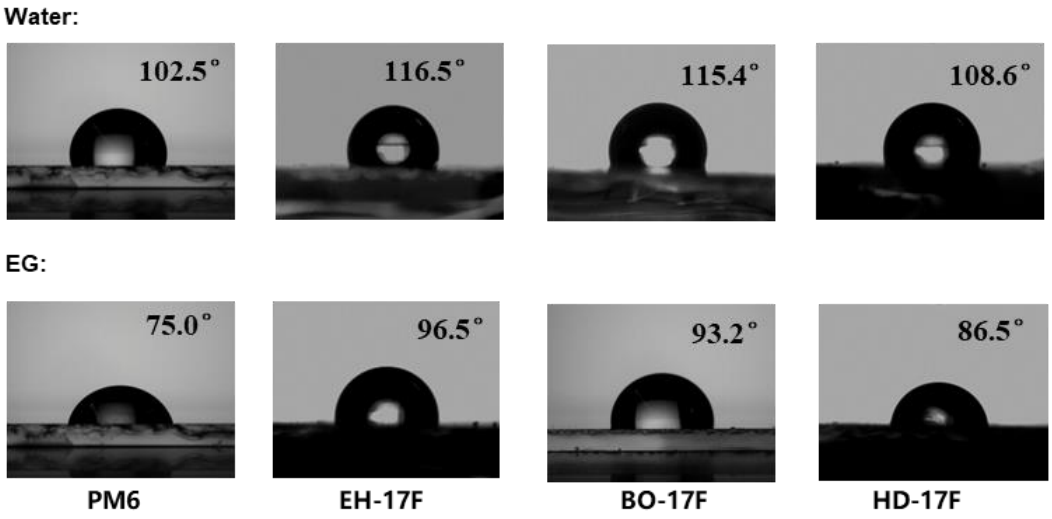

Figure S10. Contact angles of the corresponding pure films of PM6, EH-17F, BO-17F, and HD-17F.

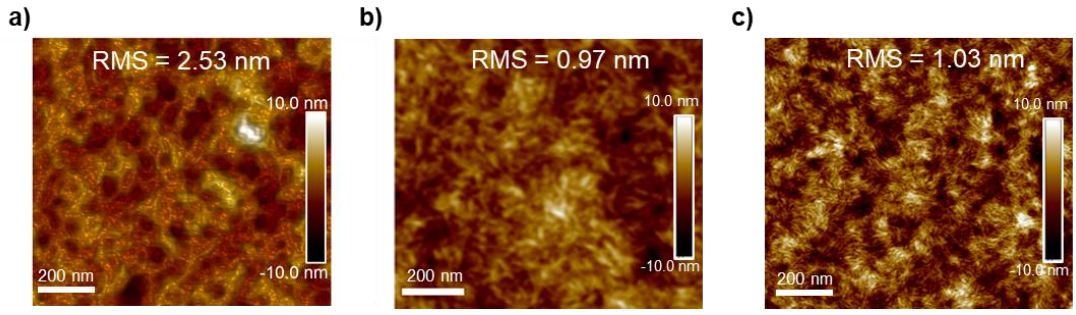

Figure S11. AFM images for (a) PM6:EH-17F, (b) PM6:BO-17F, (c) PM6:HD-17F.

Materials and synthesis

All chemicals, unless otherwise specified, were purchased from Aldrich or other commercial resources and used as received. Toluene was distilled from sodium benzophenone under nitrogen before using.

^{1}H and ^{13}C NMR spectra were recorded on Bruker AV-400 MHz NMR spectrometer or Bruker AV-600 MHz NMR spectrometer. Chemical shifts are reported in parts per million (ppm, δ). ^{1}H NMR and ^{13}C NMR spectra were referenced to tetramethylsilane (0 ppm) for $CDCl_3$. Mass spectra were collected on a MALDI Micro MX mass spectrometer, or an API QSTAR XL System.

Synthesis of compound 2a: To a two-neck flask containing compound 1 (558 mg, 0.7 mmol), 3-(bromomethyl)hexane (199 mg, 1.1 mmol), 3-(perfluorooctyl)propyliodide (410 mg, 0.7 mmol), KI (124 mg, 0.75 mmol), K_2CO_3 (491 mg, 3.6 mmol), and dried DMF (15 ml) were added under N_2 atmosphere. The reaction was stirred at 100 ℃ for 12 h. After cooling to room temperature, the reaction was extracted with ethyl acetate three times. The organic layers were combined and washed with saturated brine, and dried over Na_2SO_4. After evaporation of the solvent, the residue was purified by column chromatography (PE/DCM = 10/1) to give the corresponding product 2 as an orange oil in 30% yield (364 mg).

^{1}H NMR (400 MHz, $CDCl_3$) δ7.02 (s, 2H), 4.76-4.63 (m, 2H), 4.58-4.57 (m, 2H), 2.81 (d, J = 7.6 Hz, 4H), 2.18 (d, J = 5.5 Hz, 2H), 2.08-1.95 (m, 3H), 1.86-1.81 (m, 4H), 1.44 -1.24 (m, 34H), 1.09-1.05 (m, 2H), 1.01-0.95 (m, 1H), 0.90-0.84 (m, 9H), 0.61 (m, 6H).

Synthesis of Compound 2b: The detailed synthetic procedure of compound 2b was similar to that of compound 2a. The little difference is that the 3-(bromomethyl)hexane used in the synthetic procedure of compound 2a was replaced with 5-(Bromomethyl)undecane (434 mg, 0.74 mmol). The final product compound 2b was obtained as an orange solid (273 mg, 40%).

^{1}H NMR (600 MHz, $CDCl_3$) δ7.03 (s, 2H), 4.72-4.69 (m, 2H), 4.60-4.55 (m, 2H), 2.85 (t, J = 7.6 Hz, 4H), 2.81 (d, J = 5.5 Hz, 2H), 2.15-1.87 (m, 2H), 1.86-1.84 (m, 4H), 1.43 -1.27 (m, 36H), 1.07-0.97 (m, 3H), 1.01-0.94 (m, 6H), 0.89-0.86 (m, 9H), 0.67 (m, 7H).

^{13}C NMR (151 MHz, $CDCl_3$) δ 147.55, 147.29, 142.54, 142.28, 137.07, 136.99, 136.95, 136.74, 131.25, 131.03, 123.60, 123.57,122.99, 122.94, 119.55, 119.39, 118.19, 118.08, 117.98, 116.31, 116.16, 112.47, 112.09, 111.62, 110.82, 110.66, 110.45, 108.01, 106.67, 54.66, 50.04, 38.77, 31.95, 31.51, 29.71, 29.70, 29.66, 29.64, 29.62, 29.59, 29.54, 29.50, 29.47, 29.38, 29.30, 28.81, 28.77, 25.23, 22.71, 22.59, 22.43, 21.92, 14.11, 13.88, 13.84, 13.64.

Synthesis of Compound 2c: The detailed synthetic procedure of compound 2c was similar to that of compound 2a. The little difference is that the 3-(bromomethyl)hexane used in the synthetic procedure of compound 2a was replaced with 7-(bromomethyl)pentadecane (293 mg, 0.5 mmol). The final product compound 2b was obtained as an orange solid (260 mg, 30%).

^{1}H NMR (600 MHz, $CDCl_3$) δ7.03 (s, 2H), 4.72-4.69 (m, 2H), 4.60-4.55 (m, 2H), 2.85 (t, J = 7.6 Hz, 4H), 2.81 (d, J = 5.5 Hz, 2H), 2.15-1.87 (m, 3H), 1.86-1.84 (m, 4H), 1.43

-1.27 (m, 36H), 1.07-0.97 (m, 2H), 1.01-0.94 (m, 6H), 0.89-0.86 (m, 15H), 0.67 (m, 9H).

^{13}C NMR (151 MHz, $CDCl_3$) δ 147.62, 147.60, 147.33, 142.62, 142.32, 137.11, 137.03, 137.00, 136.79, 136.77, 131.31, 131.11, 131.03, 123.69, 123.57, 123.09, 123.07 , 122.99, 122.94, 119.57, 119.45, 118.19, 118.08, 117.98, 116.31, 116.16, 112.47, 112.24, 111.65, 111.63, 110.98, 110.96, 110.45, 110.44, 54.60, 50.07, 38.77, 31.95, 31.78, 29.71, 29.70, 29.66, 29.55, 29.51, 29.49, 29.47, 29.50, 29.47, 29.38, 29.32, 29. 14, 25.46, 25.44, 22.71, 22.59, 22.47, 21.81, 14.14, 14.10, 13.94.

Synthesis of compound 3a: Under N_2 atmosphere, $POCl_3$ (1 mL) was slowly added to dried DMF (2 mL) in a two-neck flask. After stirring at 0 ℃ for 0.5 h, a solution of compound 2a (159 mg, 0.12 mmol) in dried DCM (6 mL) was added to the reaction mixture and stirred for 12 h at 80 ℃. The reaction mixture was poured into K_2CO_3 aqueous solution (10 mL) slowly and then extracted with ethyl acetate three times. The organic layers were combined and washed with saturated brine, and dried over Na_2SO_4. After evaporation of the solvent, the residue was purified by column chromatography (PE/DCM = 2/1) to give the corresponding product 3 as an orange solid in 85% yield (165 mg).

^{1}H NMR (400 MHz, $CDCl_3$) δ 10.15 (s, 2H), 4.78-4.71 (m, 2H), 4.62 (d, J = 7.5 Hz, 2H), 3.18 -3.14 (m, 4H), 2.10 (d, J = 7.8 Hz, 2H), 2.04-1.87 (m, 7H), 1.46-1.26 (m, 34H), 1.08-0.94 (m, 13H), 0.79 (t, J = 7.4 Hz, 3H), 0.58 (m, J = 7.2 Hz, 3H).

Synthesis of compound 3b:

^{1}H NMR (400 MHz, $CDCl_3$) δ 10.15 (d, 2H), 4.79-4.76 (m, 2H), 4.61-4.59 (d, J = 7.5 Hz, 2H), 3.21-3.18 (m, 4H), 2.13 (d, J = 7.8 Hz, 2H), 1.93-1.91 (m, 7H), 1.37-1.33 (m, 36H), 1.29-1.08 (m, 16H), 0.96-0.85 (t, J = 7.4 Hz, 5H), 0.60 (t, J = 7.2 Hz, 3H).

^{13}C NMR (151 MHz, $CDCl_3$) 181.70, 147.39, 147.35, 147.11, 147.08, 146.92, 146.90, 146.82, 146.67, 146.64, 143.56, 143.28, 143.25, 137.27, 137.16, 136.59, 136.58, 132.53, 132.51, 129.53, 129.51, 128.78, 128.70, 128.32, 128.28, 127.52, 127.48, 127.34, 113.00, 112.98, 112.96, 112.95, 112.75, 112.45, 112.42, 112.16, 54.99, 54.76, 50.29, 39.03, 31.90, 31.45, 29.65, 29.63, 29.60, 29.52, 29.37, 29.36, 29.33, 29.27, 25.13, 25.06, 22.41, 22.35, 22.05, 14.08, 13.87, 13.60.

Synthesis of compound 3c:

^{1}H NMR (400 MHz, $CDCl_3$) δ 10.15 (d, 2H), 4.79-4.76 (m, 2H), 4.61-4.59 (d, J = 7.5 Hz, 2H), 3.21-3.18 (m, 4H), 2.13 (d, J = 7.8 Hz, 2H), 1.93-1.91 (m, 7H), 1.37-1.33 (m, 45H), 1.29-1.08 (m, 16H), 0.96-0.85 (t, J = 7.4 Hz, 4H), 0.60 (t, J = 7.2 Hz, 3H).
^{13}C NMR (151 MHz, $CDCl_3$) 181.72, 147.39, 147.35, 147.11, 147.08, 146.93, 146.90, 146.82, 146.68, 146.57, 143.53, 143.28, 143.21, 137.28, 137.16, 136.75, 136.67, 136.59, 132.79, 132.54, 132.39, 129.54, 129.49, 128.79, 128.70, 128.35, 128.32, 127.55, 127.48, 127.34, 113.09, 113.00, 112.98, 112.96, 112.95, 112.75, 112.45, 112.44, 112.16, 54.91, 54.76, 50.29, 39.04, 31.91, 31.74, 29.68, 29.61, 29.54, 29.52, 29.38, 29.37, 29.34, 29.27, 25.39, 25.37, 22.69, 22.57, 22.46, 22.02, 14.11, 14.08, 13.92.

Synthesis of EH-17F: To a two-neck flask containing compound 3 (72.5 mg, 0.054 mmol), 2-(5,6-difluoro-3-oxo2,3-dihydro-1H-inden-1-ylidene) malononitrile (48 mg, 0.24 mmol), $CHCl_3$ (8 mL) and pyridine (0.8 mL) were added under nitrogen atmosphere. The mixture was stirred at 30 ℃ for 2 h. After evaporation of the solvent, the residue was purified by column chromatography (PE/DCM = 1/1) to give the corresponding product EH-17F as a dark solid in 65% yield (78 mg).
^{1}H NMR (600 MHz, $CDCl_3$) δ 8.77 (s, 1H), 8.59 (s, 1H), 8.37-8.35 (t, 2H), 7.63-7.60 (t, 1H), 7.54-7.42 (t, 1H), 4.82-4.57 (m, 4H), 3.00-2.68 (s, 8H), 1.88-1.54 (m, 5H), 1.44-1.26 (m, 33H), 1.04-0.55(m,18H).
HR-MS (MALDI-TOF) m/z calcd. for ($C_{85}H_{75}F_{21}N_8O_2S_5$): 1798.4281. Found: 1798.4255.

Synthesis of BO-17F:
^{1}H NMR (400 MHz, $CDCl_3$) δ 8.83 (s, 1H), 8.66 (s, 1H), 8.40-8.35 (t, 2H), 7.63-7.59 (t, 1H), 7.54-7.45 (t, 1H), 4.82-4.54 (m, 4H), 3.01-2.94 (m, 4H), 2.70 (s, 4H), 2.11-2.03 (m, 1H), 1.95-1.71 (m, 4H), 1.46 -1.45 (d, 4H), 1.34-1.27 (m, 34H), 0.87-0.85(m,15H), 0.63-0.58 (m, 7H).
^{13}C NMR (151 MHz, $CDCl_3$) δ157.74, 157.24, 155.19, 155.16, 153.62, 153.43, 153.41, 153.38, 153.32, 146.97, 146.91, 145.20, 145.01, 136.69, 136.66, 136.35, 136.66, 134.66, 134.35, 134.30, 134.23, 133.69, 133.65, 133.36, 132.88, 132.39, 132.00, 130.86, 130.57, 119.81, 119.77, 114.91, 114.76. 114.72, 114.71, 114.59, 114.57, 114.44, 114.34, 114.25, 113.31, 113.18, 112.22, 112.10, 111.67, 111.65, 111.54, 69.46,

69.45, 68.85, 55.13, 55.09, 50.56, 39.37, 31.94, 31.42, 31.00, 30.77, 30.55, 29.86, 29.78, 29.66, 29.64, 29.51, 29.42, 29.37, 29.22, 23.08, 22.71, 22.62, 22.35, 14.13, 13,84, 13.54. HR-MS (MALDI-TOF) m/z calcd. for ($C_{89}H_{83}F_{21}N_8O_2S_5$): 1854.4907. Found:1854.4415.

Synthesis of HD-17F:

^{1}H NMR (400 MHz, $CDCl_3$) δ 8.79 (s, 1H), 8.58 (s, 1H), 8.40-8.35 (t, 2H), 7.63-7.59 (t, 1H), 7.54-7.45 (t, 1H), 4.82-4.52 (m, 4H), 3.01-2.94 (m, 4H), 2.75 (s, 4H), 2.01-1.94 (m, 1H), 1.95-1.71 (m, 5H), 1.47 -1.45 (d, 5H), 1.34-1.27 (m, 34H), 0.87-0.85(m,20H), 0.63-0.58 (m, 8H).

^{13}C NMR (151 MHz, $CDCl_3$) δ157.81, 157.12, 155.09, 154.97, 153.65, 153.42, 153.41, 153.38, 153.32, 146.94, 146.71, 145.19, 145.02, 136.66, 136.60, 136.29, 134.67, 134.66, 134.35, 134.30, 134.28, 133.97, 133.61, 133.37, 132.88, 132.35, 132.00, 130.89, 130.55, 119.78, 119.74, 114.71, 114.44. 114.72, 114.71, 114.59, 114.57, 114.44, 114.34, 114.25, 113.31, 113.17, 112.24, 112.11, 111.67, 111.65, 111.54, 69.36, 69.45, 68.84, 55.13, 55.00, 50.53, 39.38, 31.95, 31.76, 31.01, 30.77, 30.55, 29.91, 29.79, 29.68, 29.65, 29.52, 29.24, 29.37, 29.10, 23.08, 22.72, 22.62, 22.35, 14.06, 13,94, 13,85, 13.64.

HR-MS (MALDI-TOF) m/z calcd. for ($C_{93}H_{91}F_{21}N_8O_2S_5$): 1910.5533. Found: 1910.5504.

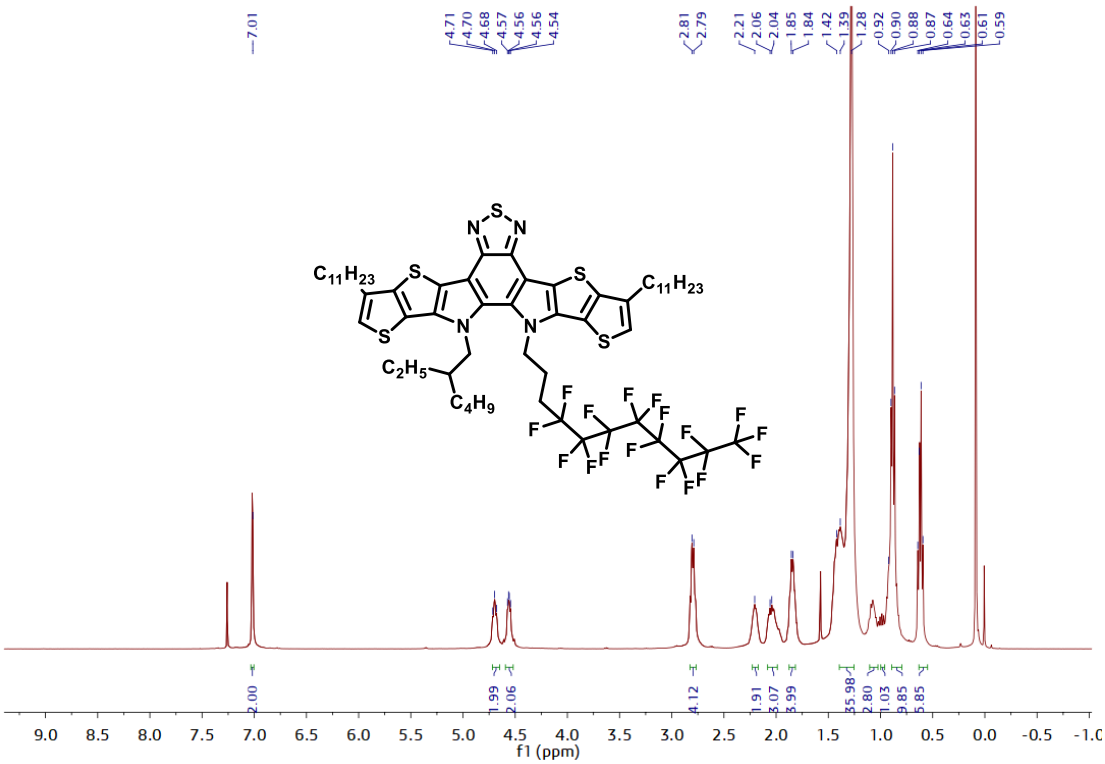

Figure S12. ^{1}H NMR spectrum of Compound 2a

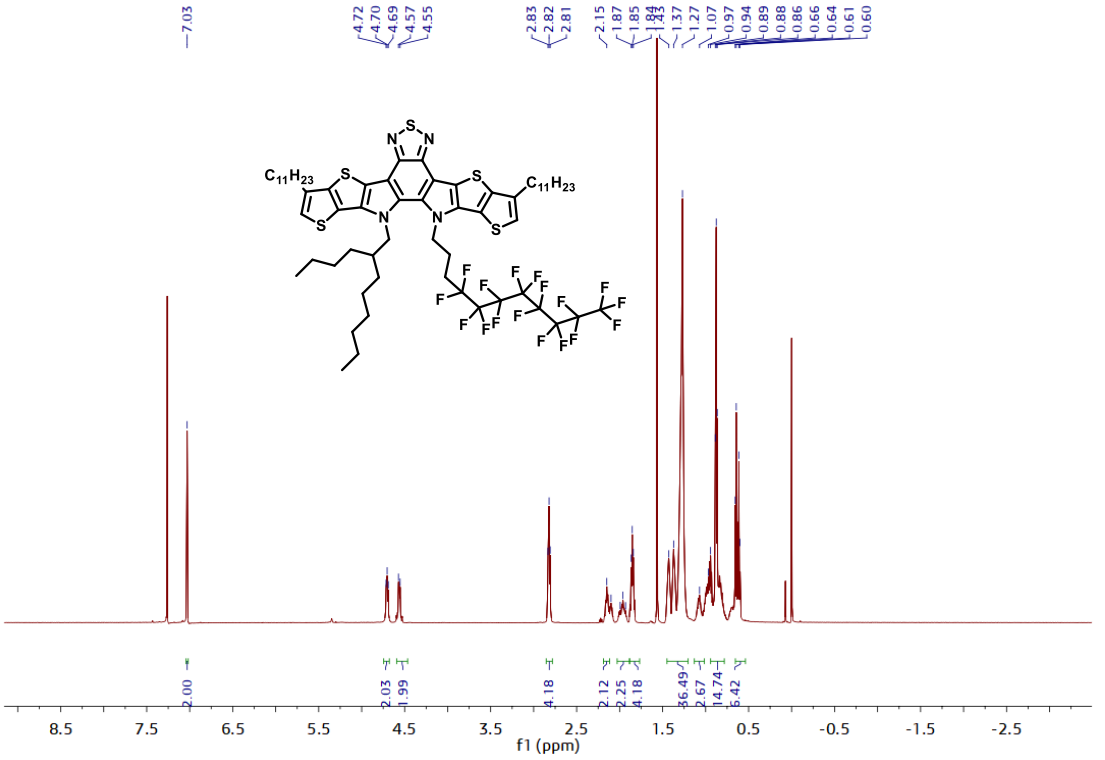

Figure S13. ^{1}H NMR spectrum of Compound 2b

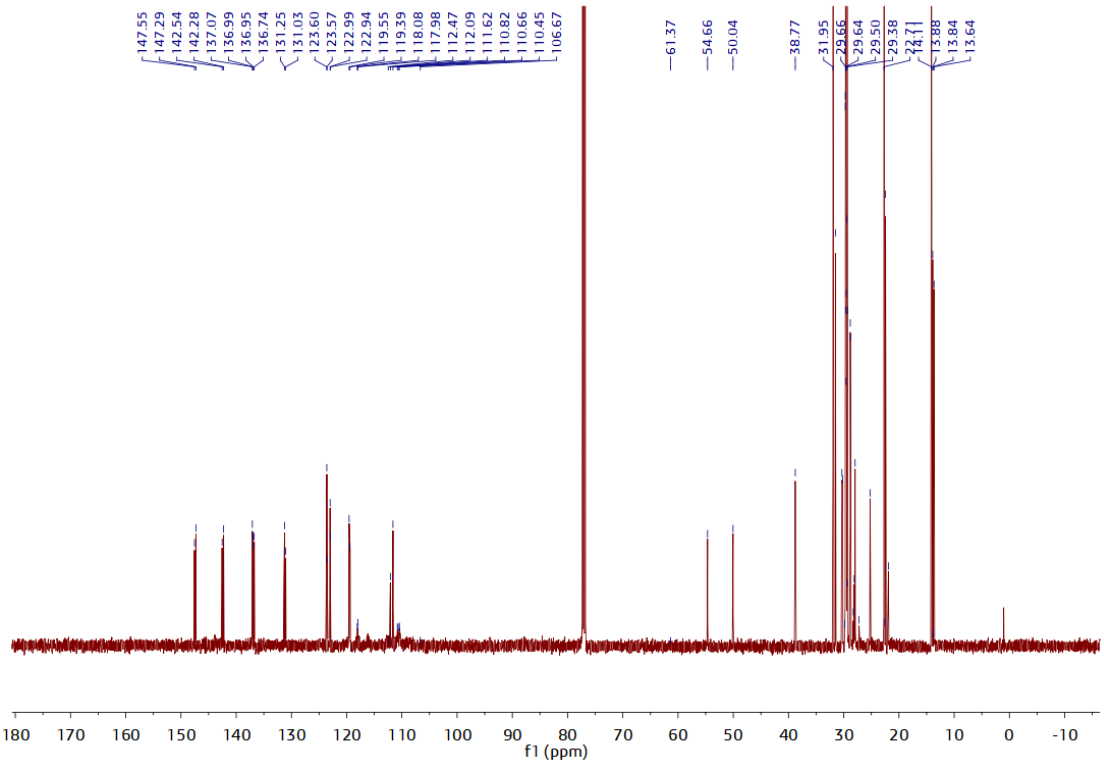

Figure S14. ^{13}C NMR spectrum of Compound 2b

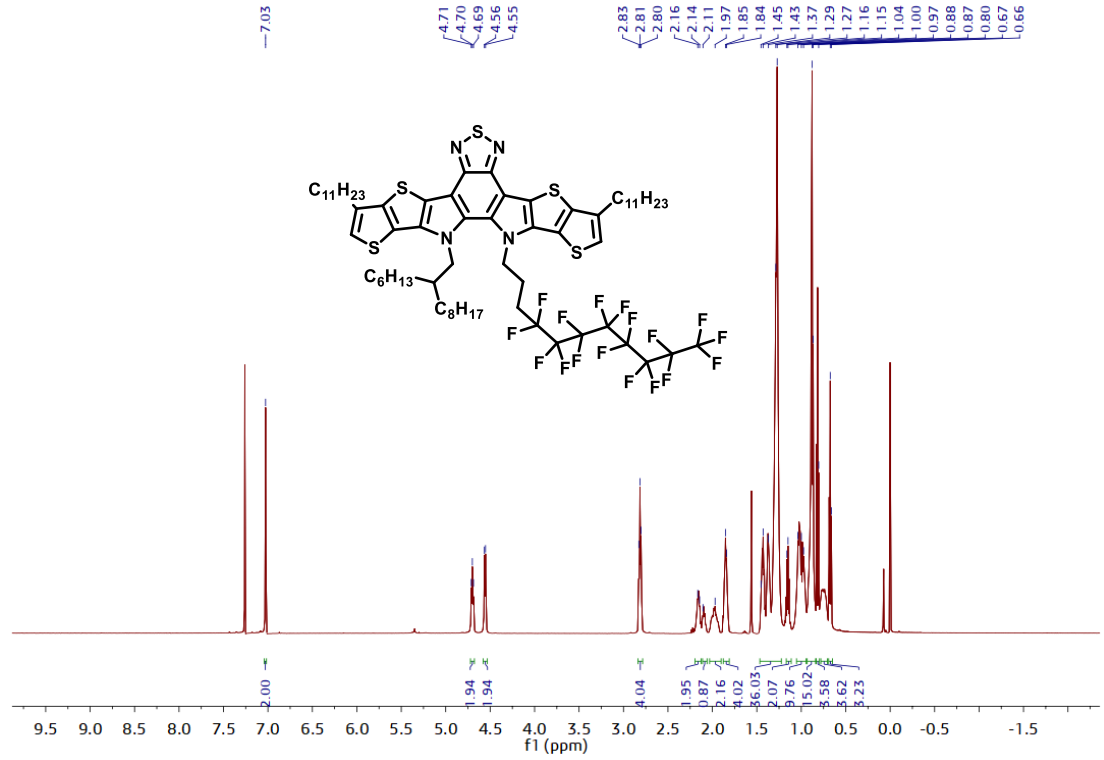

Figure S15. ^{1}H NMR spectrum of Compound 2c

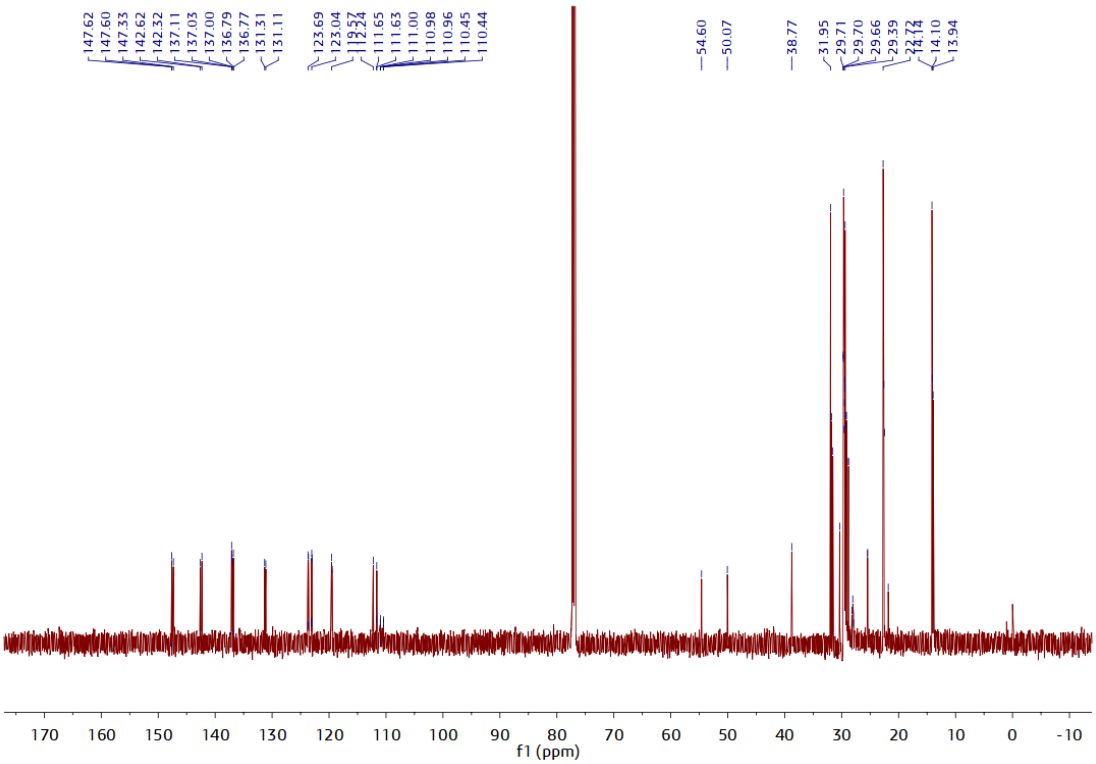

Figure S16. ^{13}C NMR spectrum of Compound 2c

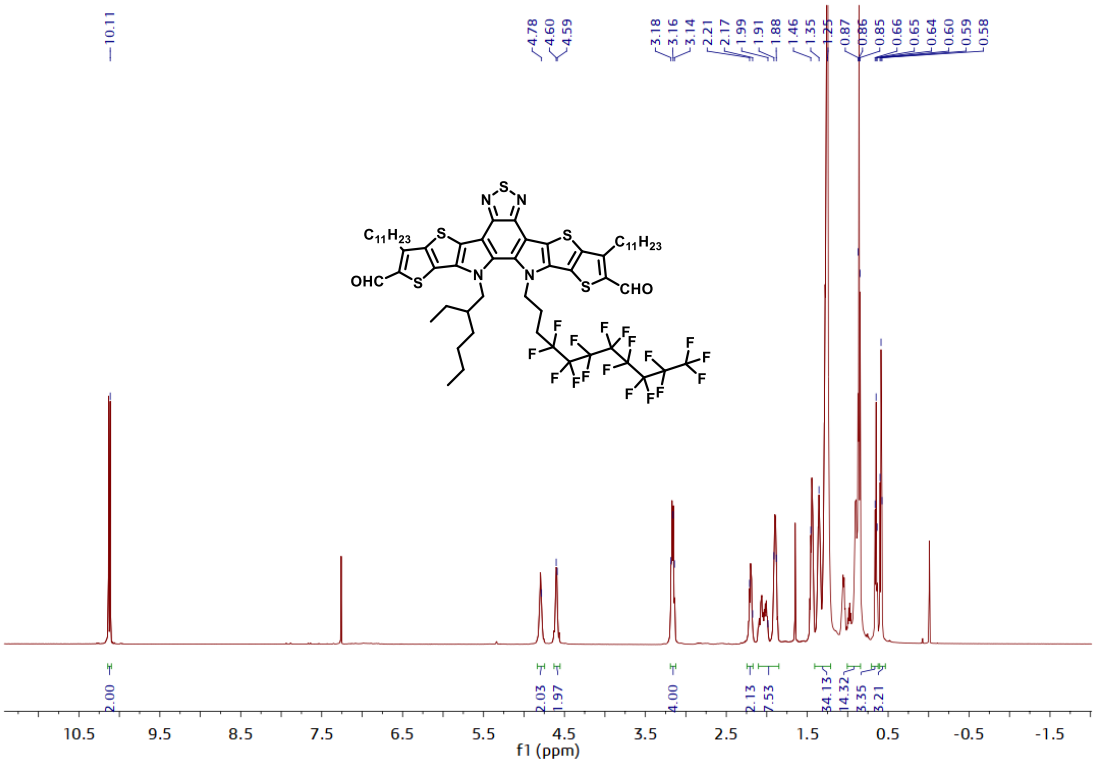

Figure S17. ^{1}H NMR spectrum of Compound 3a

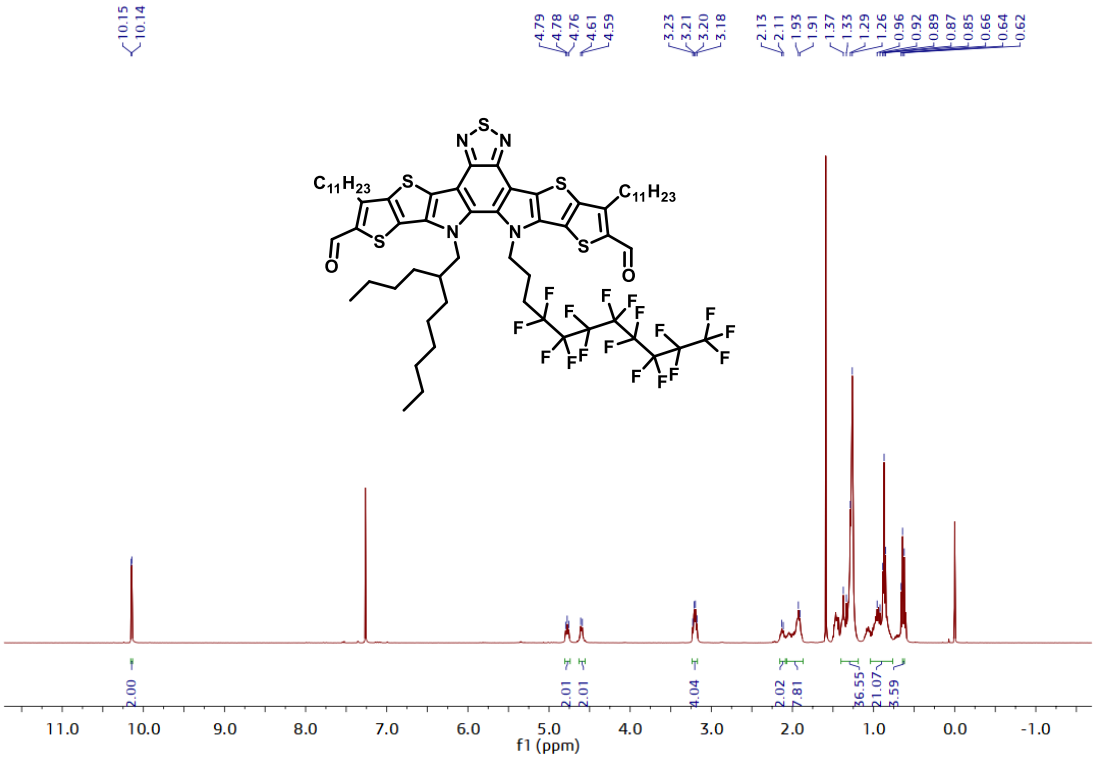

Figure S18. ^{1}H NMR spectrum of Compound 3b

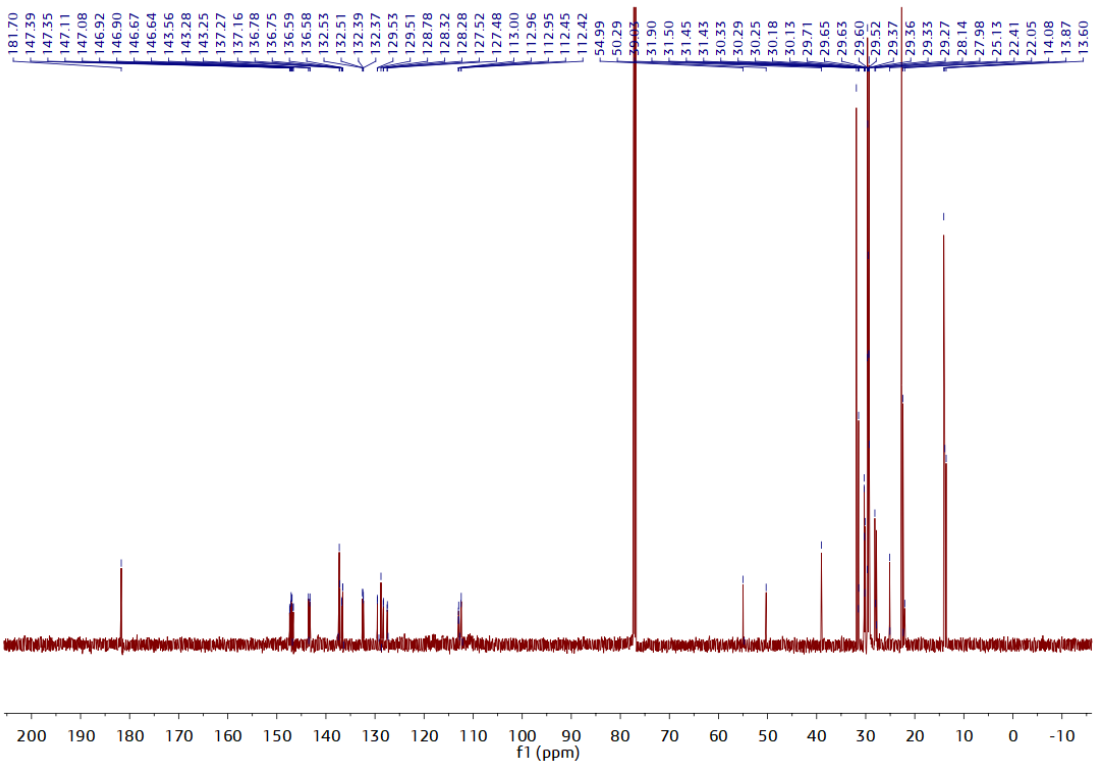

Figure S19. ^{13}C NMR spectrum of Compound 3b

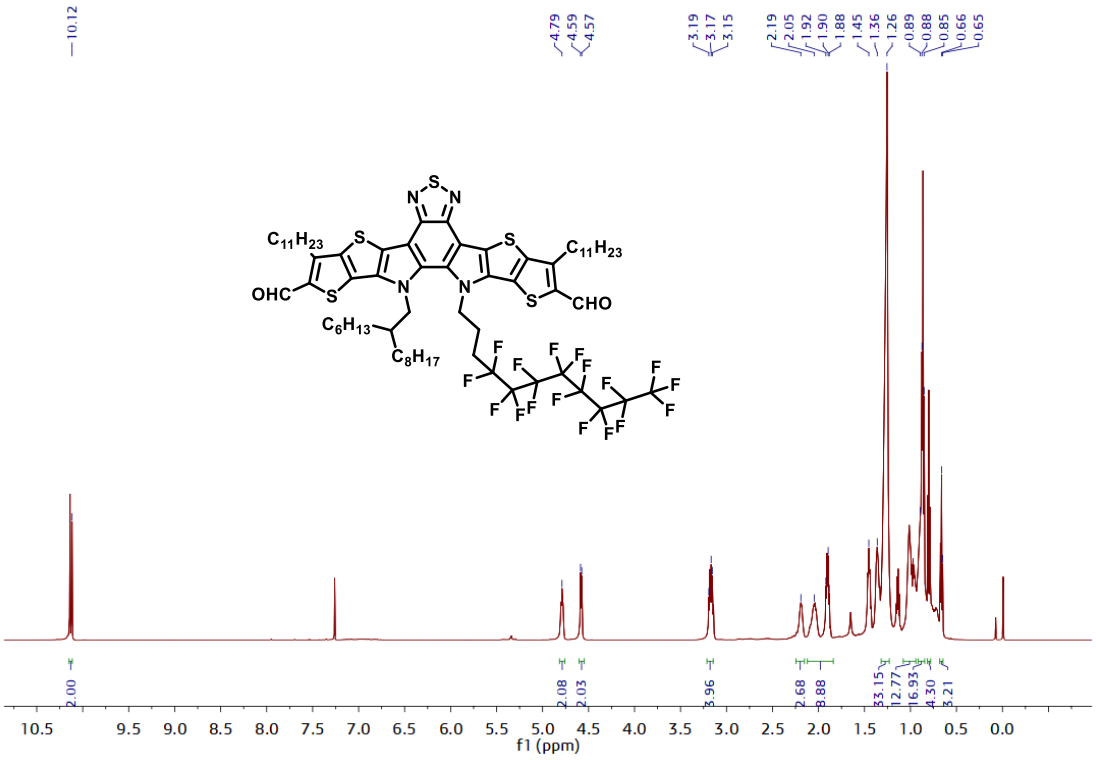

Figure S20. ^{1}H NMR spectrum of Compound 3c

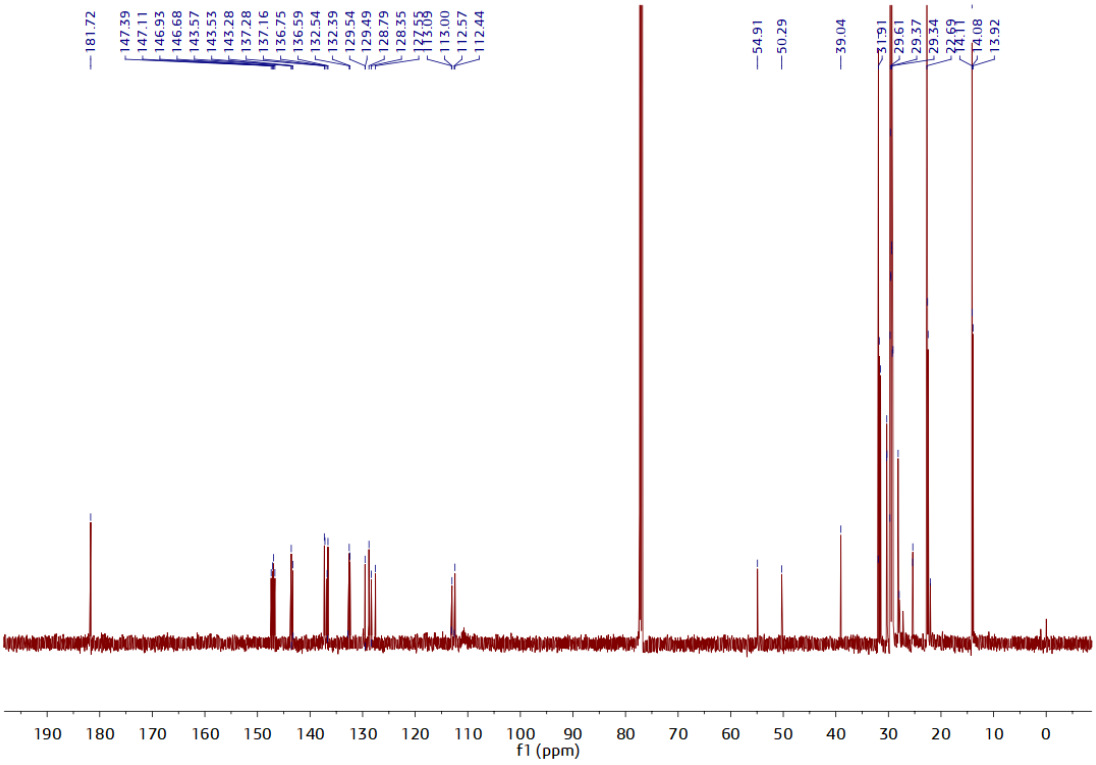

Figure S21. ^{13}C NMR spectrum of Compound 3c

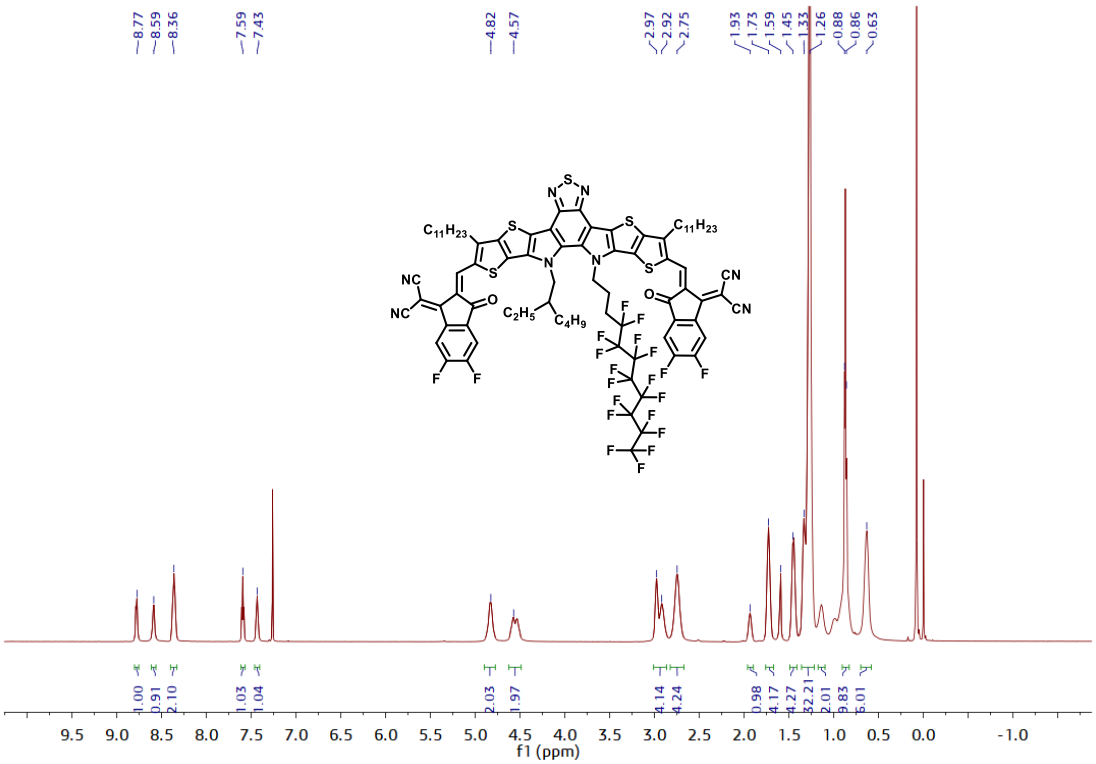

Figure S22. ^{1}H NMR spectrum of EH-17F

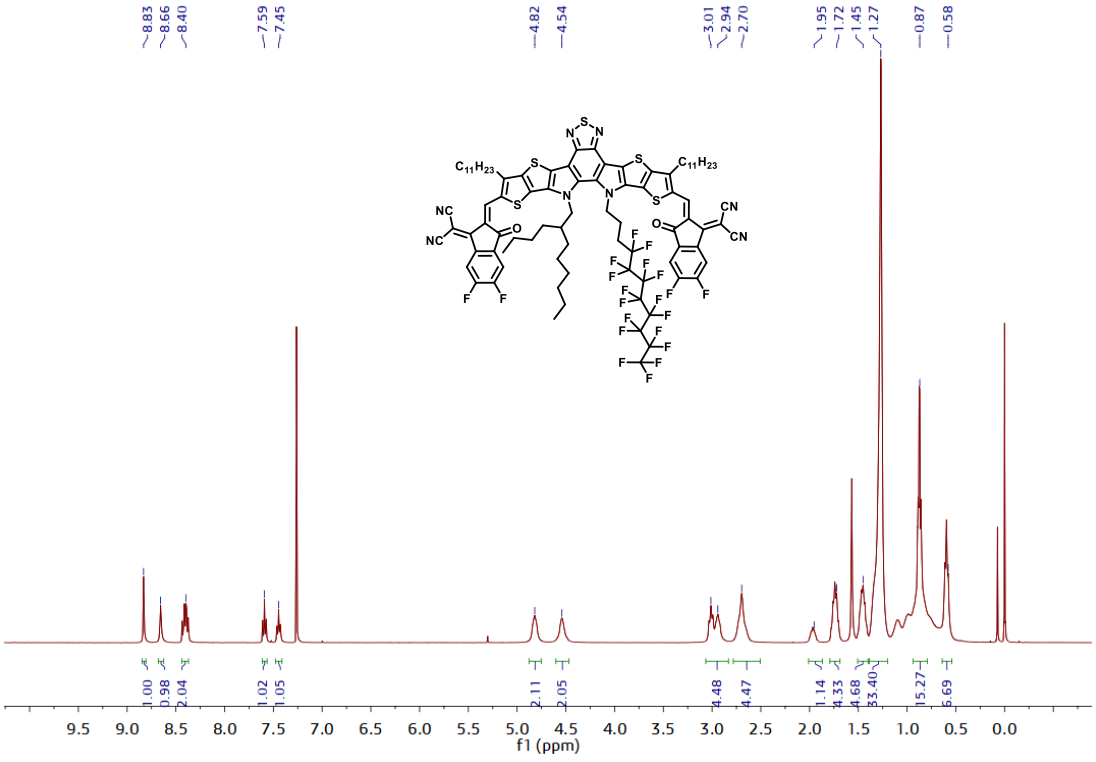

Figure S23. ^{1}H NMR spectrum of BO-17F

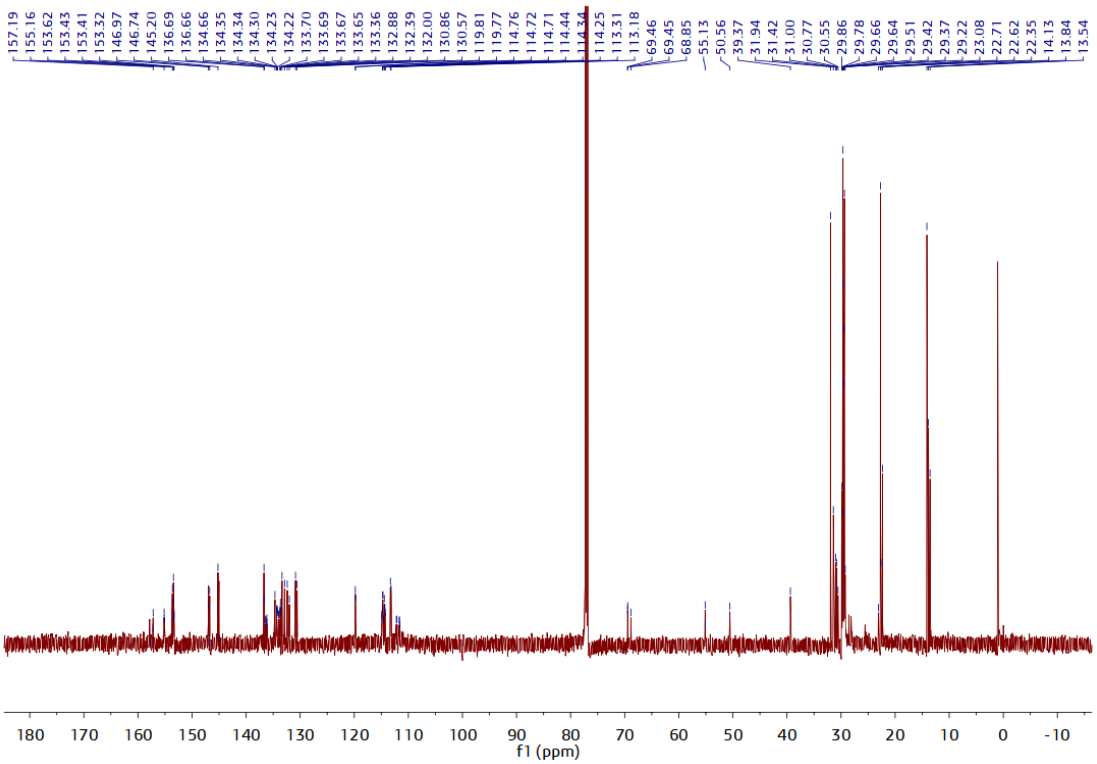

Figure S24. ^{13}C NMR spectrum of BO-17F

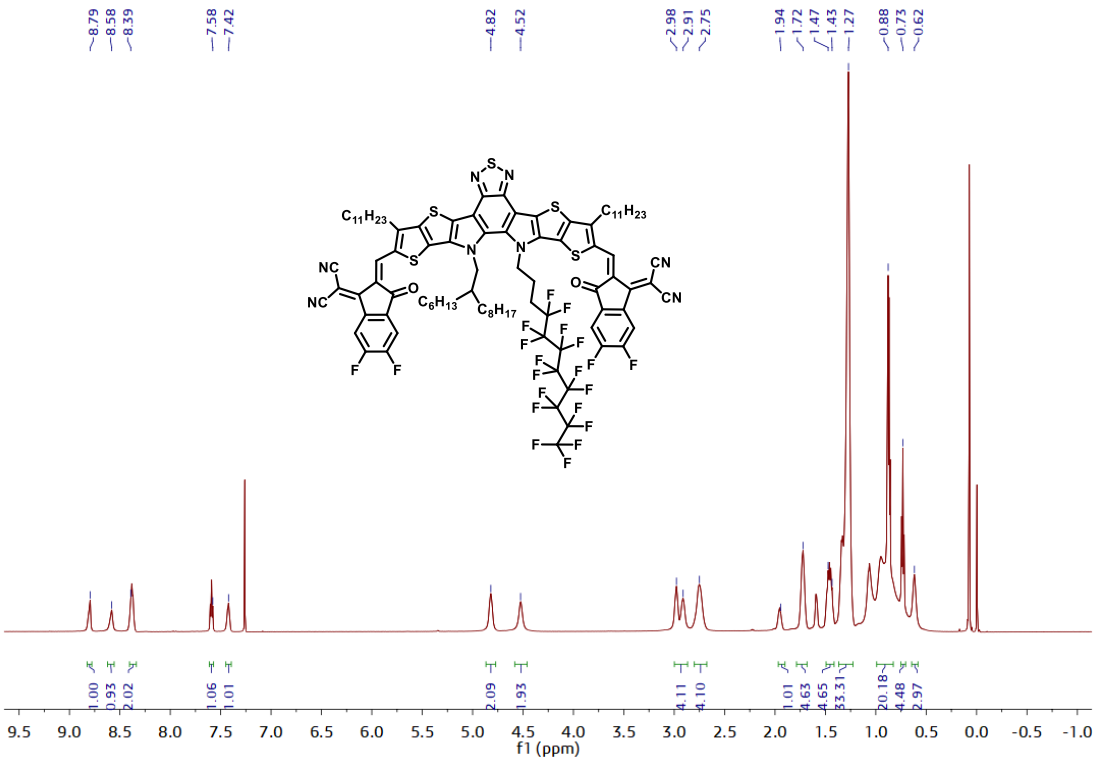

Figure S25. ^{1}H NMR spectrum of HD-17F

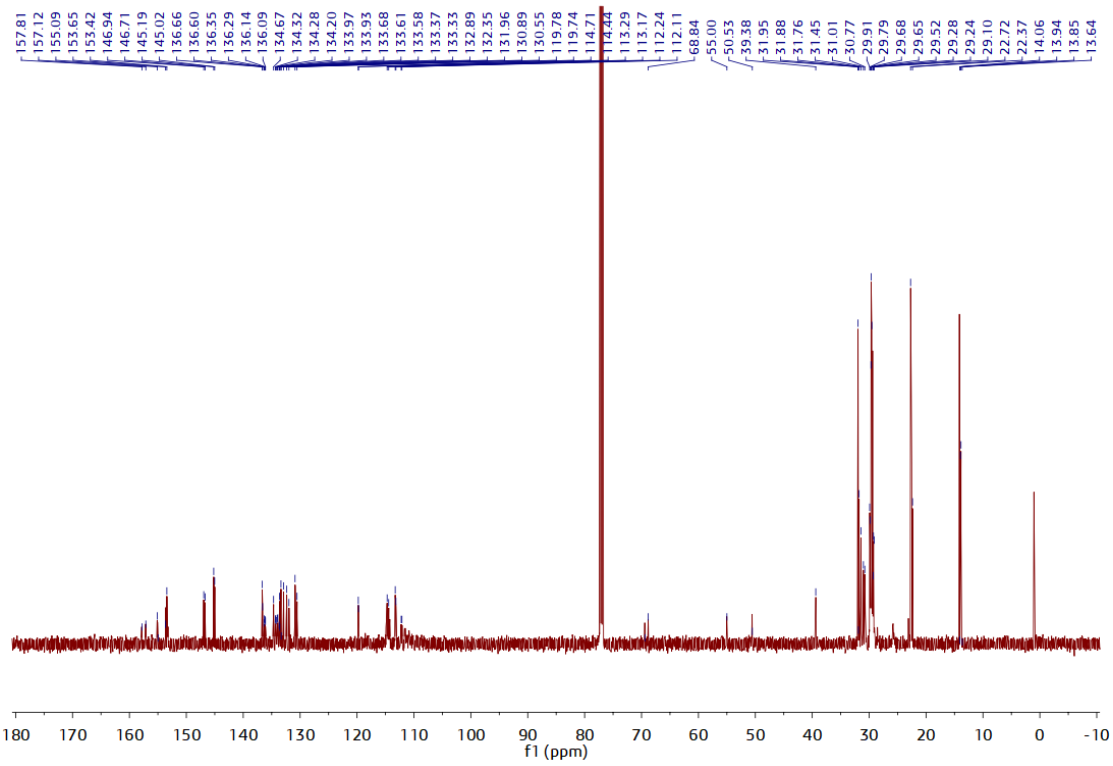

Figure S26. ^{13}C NMR spectrum of HD-17F

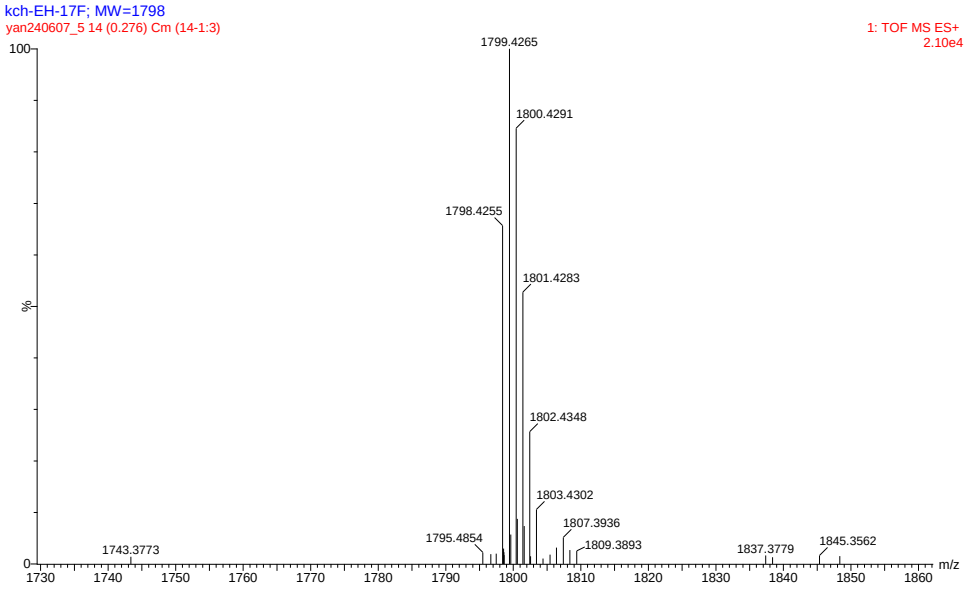

Figure S27. HR-MS spectrum of **EH-17F**

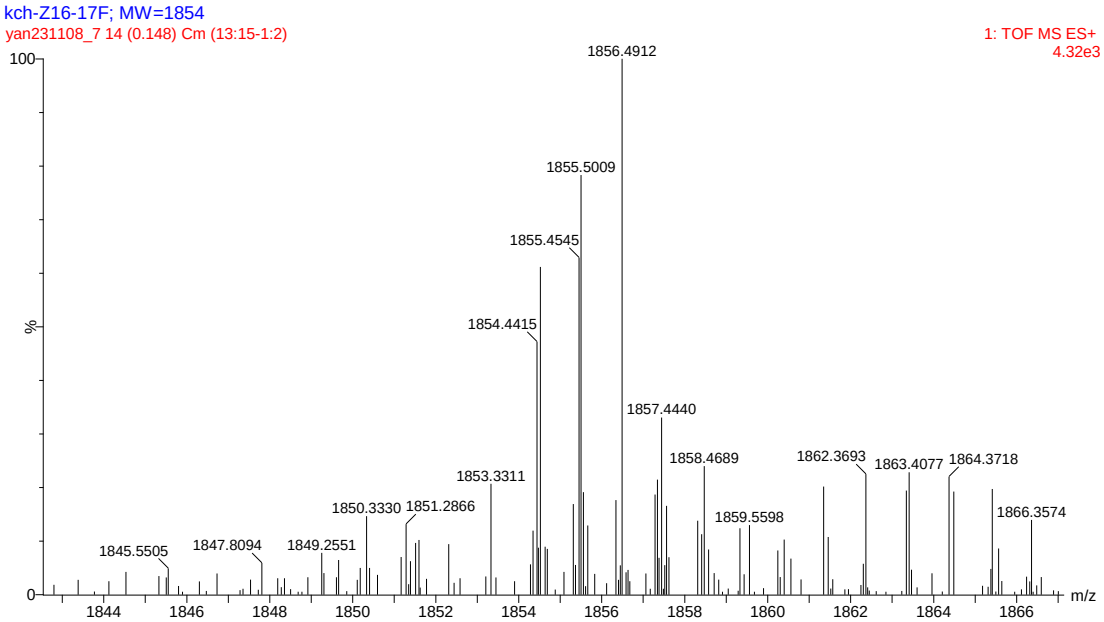

Figure S28. HR-MS spectrum of **BO-17F**

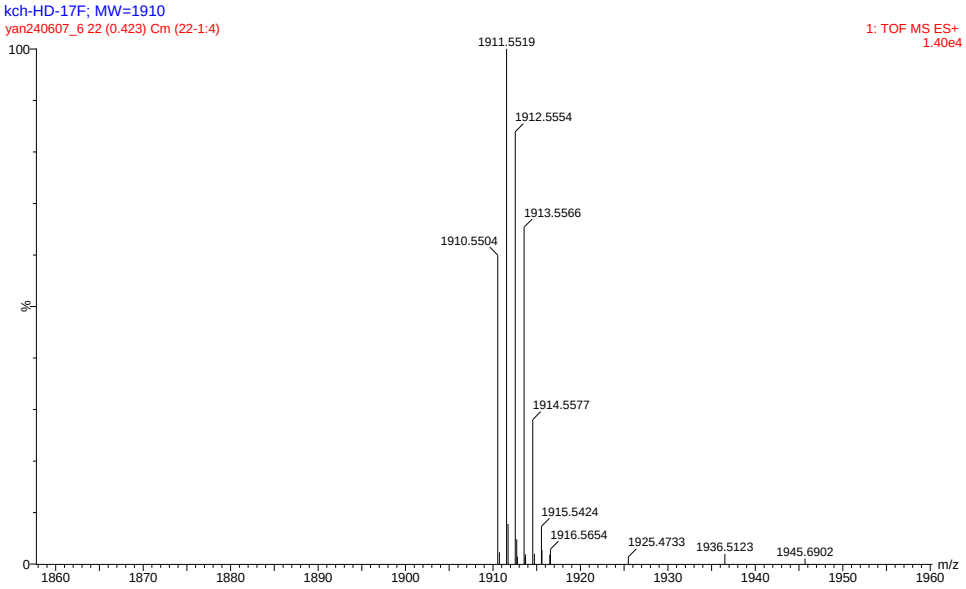

Figure S29. HR-MS spectrum of **HD-17F**

References:

1. Hexemer, A.; Bras, W.; Glossinger, J.; Schaible, E.; Gann, E.; Kirian, R.; MacDowell, A.; Church, M.; Rude, B.; Padmore, H., A SAXS/WAXS/GISAXS Beamline with Multilayer Monochromator. *J. Phys. Conf. Ser.* **2010,** *247* (1), 012007.

2. Zhang, Z.; Yang, L.; Hu, Z.; Yu, J.; Liu, X.; Wang, H.; Cao, J.; Zhang, F.; Tang, W., Charge density modulation on asymmetric fused-ring acceptors for high-efficiency photovoltaic solar cells. *Materials Chemistry Frontiers* **2020,** *4* (6), 1747-1755.